

Carboxylic acid-assisted solid-state synthesis of LiFePO_4/C composites and their electrochemical properties as cathode materials for lithium-ion batteries

George Ting-Kuo Fey · Tung-Lin Lu · Feng-Yu Wu · Wen-Hsien Li

Received: 1 July 2007 / Revised: 20 December 2007 / Accepted: 9 January 2008 / Published online: 6 February 2008
© Springer-Verlag 2008

Abstract To enhance the capability of LiFePO_4 materials, we attempted to coat carbon by incorporating various organic carboxylic acids as carbon sources. The purity of LiFePO_4 was confirmed by XRD analysis. Galvanostatic cycling, cyclic voltammetry, electric impedance spectroscopy, and conductivity measurements were used to evaluate the material's electrochemical performance. The best cell performance was delivered by the sample coated with 60 wt.% malonic acid. Its first-cycle discharge capacity was 149 mA h g^{-1} at a 0.2 C rate or 155 mA h g^{-1} at a 0.1 C rate. The presence of carbon in the composite was verified by total organic carbon and Raman spectral analysis. The actual carbon content of LiFePO_4 was 1.90 wt.% with the addition of 60 wt.% malonic acid. The LiFePO_4/C samples sintered with 60 wt.% various carboxylic acids were measured by Raman spectral analysis. The intense broad bands at 1,350 and $1,580 \text{ cm}^{-1}$ are assigned to the D and G bands of residual carbon in LiFePO_4/C composites, respectively. The peak intensity (I_D/I_G) ratio of the synthesized powders is from 0.907 to 0.935. Carbon coatings of LiFePO_4 with low I_D/I_G ratios can be produced by incorporating carboxylic acid additives before the final

calcining process. The use of carboxylic acid as a carbon source increases the overall conductivity ($\sim 10^{-4} \text{ S cm}^{-1}$) of the material.

Keywords LiFePO_4 · Carbon · Cathode · Composite · Carboxylic acid

Introduction

Lithium-ion batteries have now taken their place as the rechargeable battery of choice for portable consumer electronics equipment. Since Padhi et al. [1, 2] first reported the phosphate compound LiFePO_4 with an olivine structure in 1997, it has become of great interest, because it is environmentally benign, nonhygroscopic, cheap, abundant, and has high thermal stability and theoretical capacity of 170 mA h g^{-1} [2]. The main obstacle for this material is poor rate capability because of low electronic conductivity and low lithium-ion diffusivity through $\text{LiFePO}_4\text{--FePO}_4$ interfaces [3–6]. Recently, many researchers have been working on improving this material through different methods, such as doping to improve intrinsic conductivity [7–11], adding metal or carbon particles during synthesis [12–15], or incorporating organic or polymeric additives to form conductive carbon coatings on the particles during firing [16–18].

To enhance the capability of LiFePO_4 materials, we attempted to coat carbon by incorporating various organic carboxylic acids as carbon sources. These acids include: (a) mono-acid containing a ring structure, (b) straight-chain diacids, and (c) tri-acids. We report different carboxylic acids used to synthesize LiFePO_4 in only two steps and produce pure, well-crystallized, and homogeneous small particles of lithium iron phosphate.

Contribution to ICMAT 2007, Symposium K: Nanostructured and bulk materials for electrochemical power sources, July 1–6, 2007, Singapore.

G. Ting-Kuo Fey (✉) · T.-L. Lu
Department of Chemical and Materials Engineering,
National Central University,
Chung-Li, Taiwan 32054, Republic of China
e-mail: gfey@cc.ncu.edu.tw

F.-Y. Wu · W.-H. Li
Department of Physics, National Central University,
Chung-Li, Taiwan 32054, Republic of China

Experimental

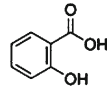
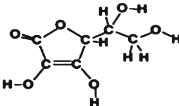
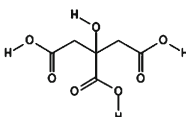
The LiFePO_4/C composite was synthesized using lithium carbonate, iron (II) oxalate dihydrate, and ammonium dihydrogen phosphate in a stoichiometric molar ratio (1.03:1:1) by a high-temperature solid-state method. The precursors were mixed by ball milling in acetone for 3 h. The resulting gel was dried at 333 K in a furnace, thoroughly reground, and heated under purified Ar/H_2 (vol. 95:5) gas for 10 h at 593 K. For the decomposed mixture, the carboxylic acid of interest dissolved in acetone was added during the grinding step, before a final heating at 873 K for 12 h under purified Ar/H_2 (vol. 95:5) gas. Table 1 lists their molecular formulas and weights. The top two are mono-acids containing a ring structure; the middle three are straight-chain di-acids; and the bottom one is tri-acid.

Coin cells of the 2032 configuration were assembled in an argon-filled VAC MO40-1 glove box in which the oxygen and water contents were maintained below 2 ppm. Lithium metal (Foote Mineral) was used as the anode and a 1-M solution of LiPF_6 in EC:DEC (1:1 v/v; Tomiyama Chemicals) was used as the electrolyte. The cathode was prepared by blade-coating a slurry of 85 wt.% LiFePO_4/C active material with 10 wt.% conductive carbon black and 5 wt.% poly(vinylidene fluoride) binder in *N*-methyl-2-pyrrolidone (NMP) on an aluminum foil current collector and dried at 393 K for 12 h. The coated cathode foil was then smoothed by pressing it through stainless-steel twin

rollers and punching out circular discs 13 mm in diameter. The cells were cycled at 0.2 C rate (with respect to a theoretical capacity of 170 mA h g^{-1}) and $298 \pm 0.5 \text{ K}$ between 2.8 and 4.0 V in a multi-channel battery tester (Maccor 4000 multi-channel battery tester). All electrochemical experiments were conducted at room temperature in a glove box (VAC, MO 40-1) filled with high-purity argon.

Structural analysis and phase purity were analyzed by a powder X-ray diffractometer (XRD), Siemens D-5000, Mac Science MXP18, equipped with a nickel-filtered $\text{Cu-K}\alpha$ radiation source ($\lambda = 1.5405 \text{ \AA}$). The diffraction patterns were recorded between scattering angles of 15° and 80° in steps of 4° min^{-1} . The surface morphology of the powders was observed with a field emission scanning electron microscope (FE-SEM; S-800). The surface carbon structure in the LiFePO_4/C composite was investigated by Raman spectroscopy (ISA T64000) in the range of $800\text{--}1,750 \text{ cm}^{-1}$. The excitation wavelength was supplied by an internal Ar-ion 10-mW laser. A total organic carbon instrument (OIA, Model Solids) was used to measure the carbon content of LiFePO_4 . The sample was then heated to 1,173 K. The carbon in the sample was converted to carbon dioxide and detected with the NDIR detector. The resulting carbon dioxide mass was proportional to the mass of total carbon in the sample. The conductivity was measured by four-point conductivity measurements of Keithley Model 2400S source meter.

Table 1 LiFePO_4 samples processed with organic acid additives

Carboxylic acid	Molecular formula		M. W. [g mol^{-1}]
Salicylic acid	$\text{C}_6\text{H}_4(\text{OH})(\text{COOH})$		138
Ascorbic acid	$\text{C}_6\text{H}_8\text{O}_6$		176
Malonic acid	$\text{HOOC-CH}_2\text{-COOH}$		104
Adipic acid	$\text{HOOC-(CH}_2)_4\text{-COOH}$		146
Sebacic acid	$\text{HOOC-(CH}_2)_8\text{-COOH}$		202
Citric acid	$\text{HOOCCH}_2\text{C(OH)(COOH)CH}_2\text{COOH}$		192

Fully charged coin cells were subjected to impedance measurements. The impedance spectra were recorded using a Schlumberger 1286 electrochemical interface and frequency response analyzer (Model 1255) driven by Corrware software (Scribner Associates). The frequency range was 65 kHz to 0.001 Hz, and the amplitude of the perturbation signal was 20 mV. The impedance spectra were analyzed with Z-view software (Scribner Associates). Phase transitions during the cycling processes were examined by a slow scan cyclic voltammetric experiment. The cells for the cyclic voltammetric studies were assembled inside a glove box with lithium metal foil serving as both counter and reference electrodes. The electrolyte used was the same as the one used in the coin cell. Cyclic voltammograms were run on a Solartron 1287 Electrochemical Interface at a scan rate of 0.1 mV s^{-1} between 2.8 and 4.2 V.

Results and discussion

X-ray diffraction

X-ray powder diffraction patterns of LiFePO_4 coated with 60 wt.% malonic acid after firing at (a) 773, (b) 873, (c) 973 K are shown in Fig. 1. All samples reveal a single-phase LiFePO_4 with an ordered olivine structure indexed by orthorhombic Pnmb (JCPDS card no. 40-1499) [7]. No impure phases of Fe_2O_3 and $\text{Li}_3\text{Fe}_2(\text{PO}_4)_3$ [19] were observed in the as-prepared LiFePO_4 . The diffraction peaks

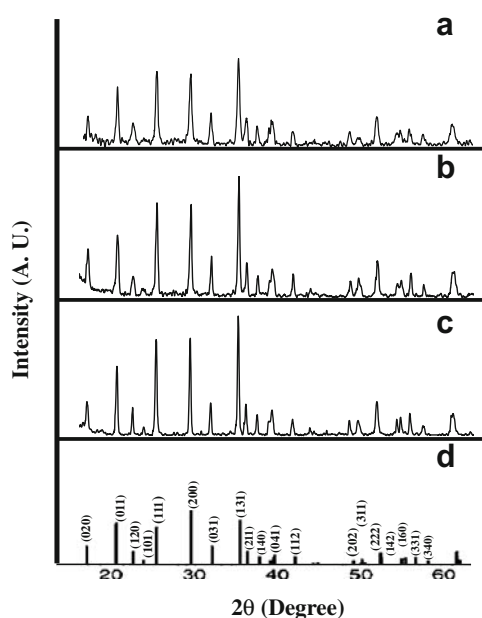


Fig. 1 X-ray powder diffraction patterns of LiFePO_4 coated with 60 wt.% malonic acid after firing at different temperatures; **a** 773 K, **b** 873 K; **c** 973 K. **d** JCPDS of LiFePO_4

became slightly sharper with increasing temperature, implying an improvement in crystallinity [20, 21]. However, no crystalline or amorphous carbons were detected in the XRD patterns, because the formed carbon was too small or too thin on LiFePO_4 .

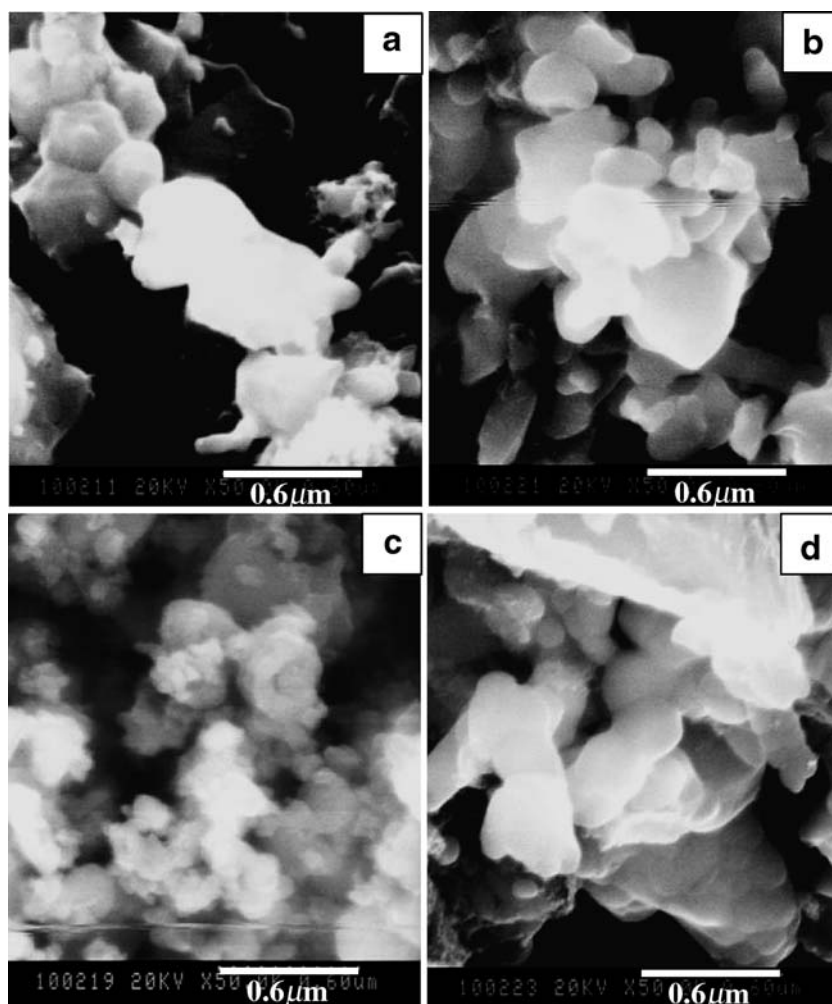
Particle morphology

Field emission scanning electron micrographs of LiFePO_4 coated with various weight percent malonic acids, (a) 0, (b) 10, (c) 60, (d) 100 wt.%, are shown in Fig. 2. The particle size decreased as more carbon was added. However, adding too much malonic acid, such as a 100-wt.% level, caused a dramatic increase in particle growth. The actual carbon content in the LiFePO_4/C composite was measured by total organic carbon analysis. The carbon-coated LiFePO_4 powder was a deep-black color, in contrast to the gray color of bare LiFePO_4 powder. Table 2 lists the carbon contents of LiFePO_4 coated with various weight percent malonic acids. The SEM observations were consistent with the results of particle-size distribution measured. Figure 3 shows the particle-size distribution of LiFePO_4 coated with 60 wt.% malonic acid. The particle-size distribution of LiFePO_4/C composite powders is mainly between 200 and 500 nm. Table 3 lists the average particle sizes based on the LiFePO_4 samples coated with 60 wt.% various carboxylic acids. Compared with the bare sample, the LiFePO_4 samples coated with 60 wt.% various carboxylic acids, all had small and uniform particle size. The use of carboxylic acid as a carbon source not only decreases particle size but also prevents particles from growing during the final sintering process [16, 18]. Details of the morphological investigation of LiFePO_4/C composites synthesized using malonic acid as a carbon source were analyzed by SEM, TEM/SAED/energy dispersive X-ray spectroscopy (EDS), and HRTEM in our recent work [22].

Carbon analysis

To gain a better understanding of the relationship between electronic conductivity, carbon content, and cell capacity, we studied LiFePO_4/C composite materials further using Raman spectroscopy, total organic carbon analysis, and four-point conductivity measurements. Recently, Doeff et al. [17, 23], Hwang et al. [7, 24], Mi et al. [25], and Salah et al. [26] reported Raman spectral analyses for LiFePO_4/C composite cathode materials. They observed that the intense broad bands at about $1,350$ and $1,580 \text{ cm}^{-1}$ are assigned to the disorder (D) and graphene (G) bands of residual carbon in LiFePO_4/C composites, respectively. Figure 4 displays the above similar band features near $1,350$ and $1,580 \text{ cm}^{-1}$ in the Raman spectra of the LiFePO_4 samples calcined with various 60 wt.% carboxylic acids.

Fig. 2 SEM micrographs of LiFePO_4 coated with various weight percent malonic acids. **a** 0 wt.%, **b** 10 wt.%, **c** 60 wt.%, **d** 100 wt.%



The G band at around $1,580\text{ cm}^{-1}$ corresponded to an ideal graphitic lattice vibration mode with E_{2g} symmetry [27], whereas the D band at around $1,350\text{ cm}^{-1}$ corresponded to a graphitic lattice vibration mode with A_{1g} symmetry [28]. The relative intensity ratio of the D band vs. G band can be used to evaluate the content of sp^3 - and sp^2 -coordinated carbon in the sample, as well as the degree of carbon disorder in microcrystalline graphite. Doeff et al. reported

Table 2 Carbon content and initial discharge capacity of LiFePO_4 coated with various weight percent malonic acids

Wt.% of malonic acid added	Carbon content (wt.%)	Initial discharge capacity (mA h g^{-1})	Conductivity σ (S cm^{-1})
10	0.81	125	2.48×10^{-5}
30	1.12	140	3.74×10^{-5}
60	1.90	149	4.18×10^{-5}
100	2.63	123	9.03×10^{-5}

that higher discharge capacities and better rate capability of LiFePO_4 cathodes are directly correlated with increased amounts of sp^2 -type carbon domains and decreased level of disorder in graphene planes [18]. Furthermore, a relatively weak band appeared at 940 cm^{-1} corresponding to the symmetric PO_4 stretching vibration of LiFePO_4 [17, 29].

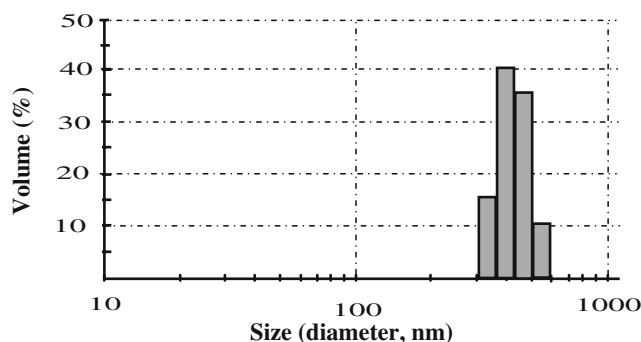


Fig. 3 Particle-size distribution of LiFePO_4 coated with 60 wt.% malonic acid

Table 3 I_D/I_G ratio, conductivity, carbon content, particle-size distribution, and initial capacity of LiFePO_4 coated with 60 wt.% various carboxylic acids

Sample	Raman band (cm^{-1})	I_D/I_G	$A_{\text{sp}^3}/A_{\text{sp}^2}$	Conductivity σ (S cm^{-1})	Average particle size (nm)	Carbon content (wt.%)	Initial capacity (mA h g^{-1})
Bare	sp^3	1,368	4.64	2.36×10^{-5}	720	0.87	1st CC=134
	sp^2	1,590	0.938				1st DC=108
Malonic acid	sp^3	1,340	3.45	4.18×10^{-5}	416	1.90	1st CC=172
	sp^2	1,602	0.918				1st DC=149
Adipic acid	sp^3	1,340	3.67	4.17×10^{-4}	477	6.75	1st CC=128
	sp^2	1,585	0.935				1st DC=104
Sebacic acid	sp^3	1,350	3.53	7.74×10^{-4}	434	7.20	1st CC=135
	sp^2	1,594	0.925				1st DC=113
Citric acid	sp^3	1,360	3.48	1.13×10^{-4}	343	12.43	1st CC=128
	sp^2	1,589	0.926				1st DC=110
Salicylic acid	sp^3	1,350	3.35	2.08×10^{-4}	414	5.20	1st CC=135
	sp^2	1,594	0.907				1st DC=116
Ascorbic acid	sp^3	1,362	3.58	5.68×10^{-5}	386	13.11	1st CC=128
	sp^2	1,585	0.928				1st DC=112

Conductivity measurements were tested at 295 K. Cells cycled between 4.0 and 2.8 V at a 0.2 C rate
 CC Charge capacity, DC discharge capacity

This confirms the presence of phosphate in the synthesized cathodes.

Table 3 lists some carbon-related properties of LiFePO_4/C composites, such as electronic conductivity, total carbon content, cell performance, particle-size distribution, and Raman spectral analysis. All data listed in this table are based on the composites coated with 60 wt.% of various carboxylic acids. It is worth noting that the cell performance shown may not be under the best conditions except for

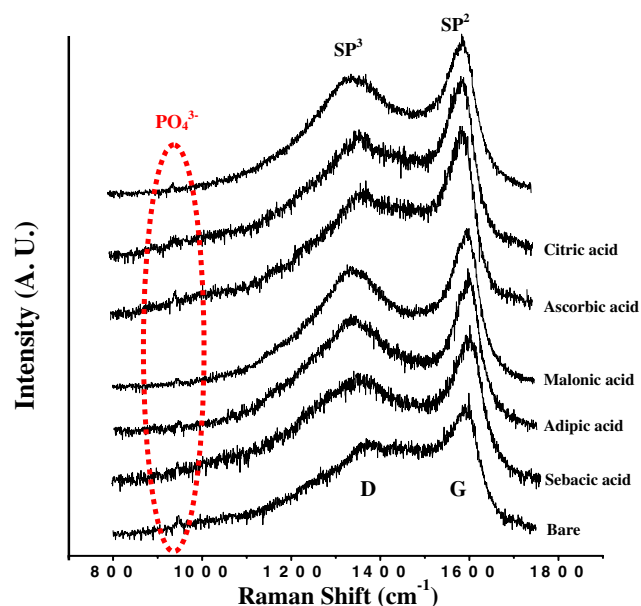


Fig. 4 Raman spectra of LiFePO_4 synthesized with various carboxylic acids

malonic acid. The Raman peak intensity and band area ratios of these D and G bands for LiFePO_4/C composites are calculated. The I_D/I_G ratios of the synthesized powders are from 0.907 to 0.935. A deconvolution analysis of the D and G bands provides the values of the individual band area and the area ratio of sp^3 - to sp^2 -coordinated carbon ($A_{\text{sp}^3}/A_{\text{sp}^2}$) in the samples. Both ratio trends of I_D/I_G and $A_{\text{sp}^3}/A_{\text{sp}^2}$ are consistent in all cases of carboxylic acids that we studied.

The electronic conductivity of these composites has a complicated correlation with the peak intensity ratio and the band area ratio of the D vs. G band. Carbon content also needs to be taken into consideration, and in some cases, can make it even more complicated. Cell performance in terms of discharge capacity and rate capability of LiFePO_4 cathodes is correlated with proper amounts of sp^2 -type carbon domains and a decreased level of disorder in graphene planes. All LiFePO_4 coated with various carboxylic acids had better conductivity than bare samples,

Table 4 Carbon content, conductivity, and initial discharge capacity of optimal carboxylic acid-coated LiFePO_4 composites

Sample	Carbon content (wt.%)	Conductivity σ (S cm^{-1})	Initial discharge capacity (mA h g^{-1})
60 wt.% malonic acid	1.90	4.18×10^{-5}	149
10 wt.% adipic acid	2.89	4.47×10^{-5}	140
40 wt.% sebacic acid	3.37	6.45×10^{-5}	127
30 wt.% citric acid	5.05	9.68×10^{-5}	138
50 wt.% salicylic acid	3.68	1.18×10^{-4}	122

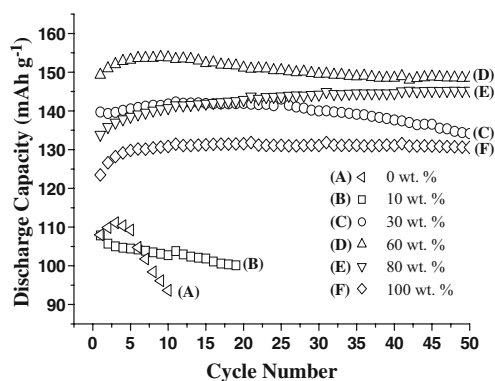


Fig. 5 Discharge behavior of LiFePO_4 coated with various weight percent malonic acids

because the conductivity of LiFePO_4/C increases when the carbon content is raised. The use of carboxylic acid as a carbon source increases the overall conductivity (an increase from 10^{-5} to 10^{-4} S cm^{-1}) of the material. However, a direct and simple correlation between discharge capacity and carbon amount cannot be obtained, because it is unlikely that carbon is evenly distributed and coated on all the particles of the phosphate (Table 4).

Electrochemical behavior

The discharge behavior of LiFePO_4 coated with various weight percent malonic acids between 2.8 and 4.0 V at a 0.2 C rate is shown in Fig. 5. Based on the discharge capacity at 50 cycles, the best coating level was 60 wt.% malonic acid, which first-cycle discharge capacity was 149 mA h g^{-1} at a 0.2 C rate. The discharge capacity gradually increased with cycling and reached its maximum at 152 mA h g^{-1} after 20 cycles, then stabilized. The first-cycle discharge capacity of the bare LiFePO_4 sample was 108 mA h g^{-1} , while the 10, 30, 60, 80, and 100 wt.%

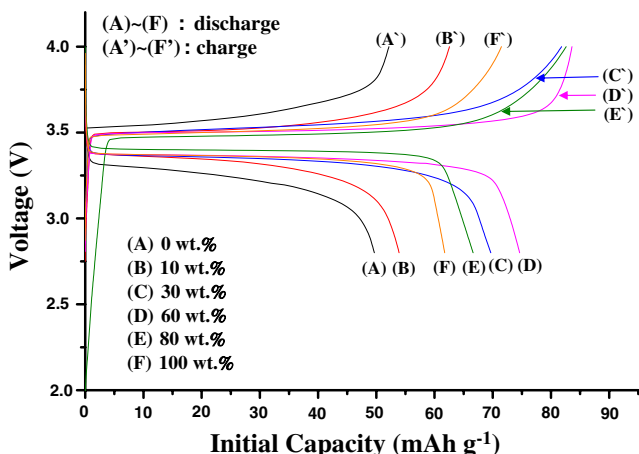


Fig. 6 Initial charge–discharge voltage profiles of LiFePO_4 coated with various weight percent malonic acids

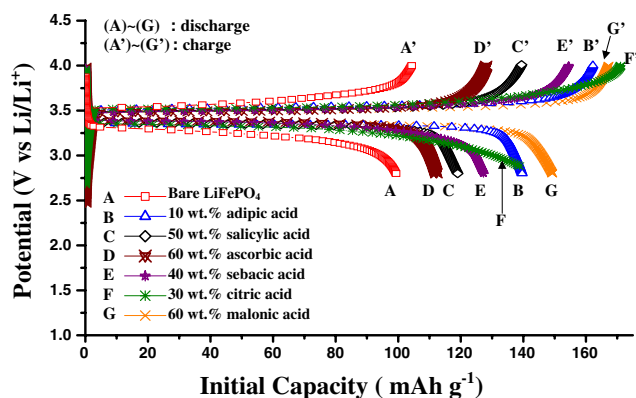


Fig. 7 Initial charge–discharge voltage profiles of optimal carboxylic acid-coated LiFePO_4/C composites

malonic acid-coated samples had first-cycle discharge capacities of 108, 140, 149, 134, and 123 mA h g^{-1} , respectively. Table 2 lists the carbon content of LiFePO_4 coated with various weight percent malonic acids. The capacity decreased more at higher coating levels because of the presence of inactive residual carbon in the electrode. Zhang et al. [30] showed that excess carbon suppresses formation of the crystalline LiFePO_4 phase. Moreover, the presence of excess coating material between the particles can decrease the active material, adversely affecting charging and discharging efficiencies.

Figure 6 presents the first-cycle charge–discharge voltage profiles for bare and LiFePO_4 powders coated with various weight percent malonic acids, which showed flat-voltage plateaus in the 3.4–3.5-V range, indicating the two-phase nature of the lithium extraction and insertion reactions between LiFePO_4 and FePO_4 [31]. The difference between the charge and discharge plateaus is only about 0.15 V, which shows that carbon-coated samples were less polarized than the bare LiFePO_4 sample. The small polarization of the composite electrodes should be attributed to the high electronic conductivity of carbon coating

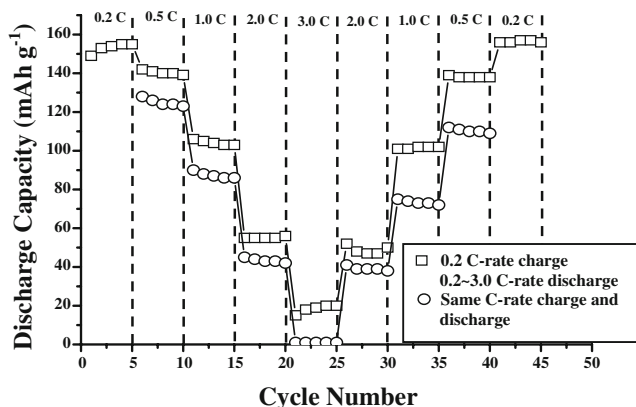


Fig. 8 Discharge performance of LiFePO_4 coated with 60 wt.% malonic acid at different discharge rates

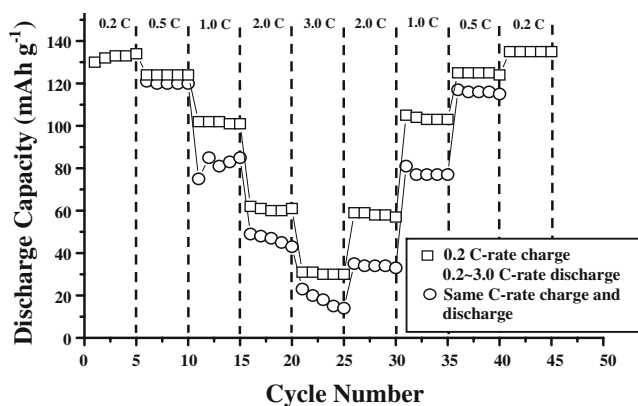


Fig. 9 Discharge performance of LiFePO₄ coated with 50 wt.% salicylic acid at different discharge rates

bestowing good electrochemical performance [2]. It is certain from Fig. 6 that LiFePO₄ coated with 60 wt.% malonic acid delivered the highest initial capacity of 149 mA h g⁻¹ amongst the carboxylic acids we studied.

Figure 7 displays the first-cycle charge–discharge voltage profiles for all optimal carboxylic acid-coated LiFePO₄

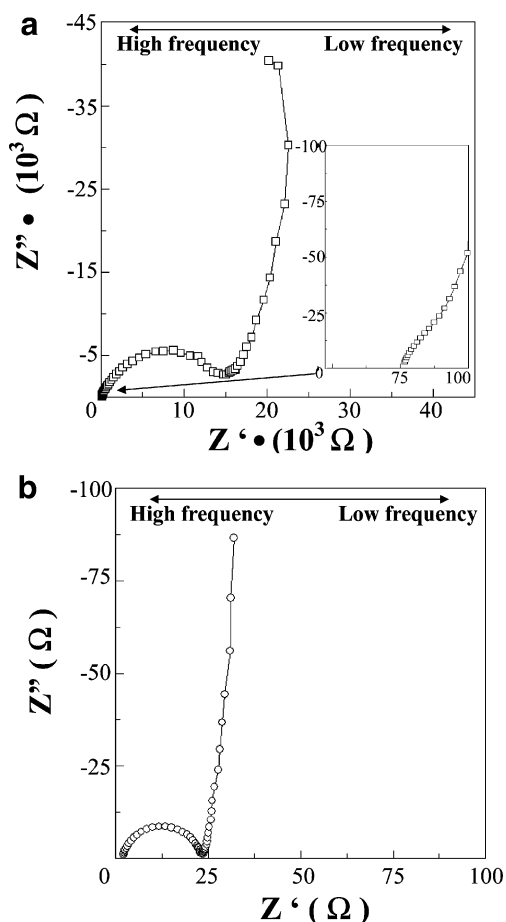


Fig. 10 Electric impedance spectra of **a** bare LiFePO₄ and **b** 60 wt.% malonic acid-coated LiFePO₄

Table 5 Electrolyte, particle-to-particle, and charge transfer resistances of bare and 60 wt.% malonic acid-coated LiFePO₄

Sample	R_e (Ω)	R_p (Ω)	R_{ct} (Ω)
Bare LiFePO ₄	76.7	15,500	110,000
60 wt.% malonic acid-coated LiFePO ₄	1.5	22	600

composites between 2.8 and 4.0 V at a 0.2 C rate. Letters from B to G stand for adipic acid, salicylic acid, ascorbic acid, sebacic acid, citric acid, and malonic acid, respectively. It can be seen that the first-cycle capacity was again the highest for the sample coated with 60 wt.% malonic acid. Similar to Fig. 6, the charge–discharge voltage profiles showed flat-voltage plateaus at the 3.4~3.5-V range with tiny polarization.

Figure 8 shows the signature curve of LiFePO₄ coated with 60 wt.% malonic acid at different discharge rates of 0.2, 0.5, 1.0, 2.0, and 3.0 C. The discharge capacity curves in the square were charged at a constant 0.2 C rate and discharged at different C rates, while the curves in the circle were charged and discharged at the same C rate. The sample discharged at different C rates delivered higher capacity than the one discharged at the same C rates. After repeated cycles, both discharge curves remained reversible in terms of their capacity trend. However, the composite cathode coated with 60 wt.% malonic acid, having an electronic conductivity of $4.18 \times 10^{-5} \text{ S cm}^{-1}$, failed when a constant 3 C rate was applied in the charge/discharge process. Because of low electronic conductivity, polarization of the electrodes becomes a key factor in determining the kinetics of the electrochemical reaction of the electrodes when they are charged and discharged at a high rate [9].

To demonstrate the electronic conductivity effect of carboxylic acid coating on the cell performance of LiFePO₄/C cathode, we performed a signature curve of LiFePO₄ coated with 50 wt.% salicylic acid, which exhibited better electronic

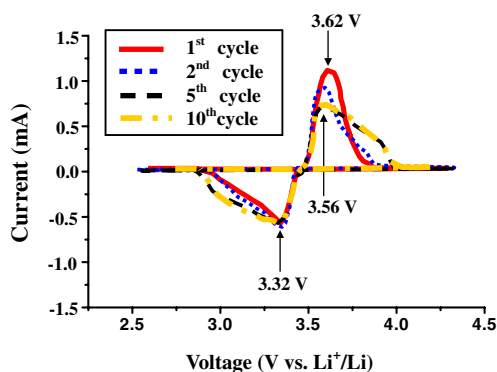


Fig. 11 Cyclic voltammograms of LiFePO₄ coated with 60 wt.% malonic acid at different cycle numbers. Scan rate = 0.1 mV s⁻¹; voltage range = 2.8~4.2 V

conductivity ($1.18 \times 10^{-4} \text{ S cm}^{-1}$) shown in Fig. 9. LiFePO_4 -coated with 50 wt.% salicylic acid did not fail at high rates when the same 3 C rate was applied in the charge–discharge process.

The Nyquist plots recorded for the bare and 60 wt.% malonic acid-coated LiFePO_4 samples are presented in Fig. 10. The electrical impedance spectroscopy of LiFePO_4 cathodes in non-aqueous electrolytes reflects processes such as the transport of lithium ions in the electrolyte, charge transfer across the electrode–electrolyte interface, and diffusion of lithium in the solid oxide matrix [32, 33]. The high-frequency semicircle represents the impedance because of a surface film on the phosphate electrode, while the low-frequency semicircle is related to a slow charge transfer process at the interface, as well as a capacitance at the film/bulk phosphate interface. The Warburg tail implies that the electrode processes under this condition are controlled by diffusion. Table 5 lists the experimental results of the electrolyte resistance (R_e), particle-to-particle resistance (R_p), charge-transfer resistance (R_{ct}), and Warburg impedance (W) for the bare and 60 wt.% malonic acid-coated LiFePO_4 samples. All resistance values of the coated sample in Table 5 decreased significantly because of effective carbon coating by malonic acid.

Figure 11 shows the cyclic voltammograms of the LiFePO_4/C composite electrode for the first, second, fifth, and tenth cycles measured between 2.8 and 4.2 V to characterize the redox reactions in Li-ion cells. The reduction and oxidation peak positions for the first, second, fifth, and tenth cycles of the LiFePO_4/C composite material are virtually the same at 3.32 and 3.56 V, respectively, which demonstrates that the $\text{Fe}^{2+}/\text{Fe}^{3+}$ redox pairs contribute to the gain and loss of electrons in LiFePO_4/C crystal structure during the lithium intercalation and de-intercalation.

It is worth noting that the cell performance of initial capacities shown in Table 3 may not be under the best conditions except for malonic acid, because all acid concentrations used for coating were kept at 60 wt.% for easy comparison with malonic acid. To extend the comparison further, Table 4 presents the conductivity results, carbon content, and initial discharge capacities of LiFePO_4 coated with five carboxylic acids at their optimum weight percent conditions. It is clearly seen from Table 4 that conductivity increased with carbon content. The LiFePO_4 sample coated with 60 wt.% malonic acid delivered the highest initial discharge capacity of 149 mA h g^{-1} even with the lowest conductivity and carbon content. Apparently, conductivity is not a key to improving the electrode properties of LiFePO_4 cathode. Carbon content needs to be taken into consideration. When carbon content increases, the ratio of the active material in the electrode decreases, leading to reduced capacity because of an

increase in inactive carbon. Discharge capacity is correlated with carbon content, which is a suitable source for a thin and uniform carbon conductive layer. According to our recent work [22], the EDS carbon map showed a uniform distribution of carbon in the sample on the surface of the composite particles. There was no remarkable segregation of carbon in the mapping area, which indicated that carbon was uniformly coated on the surface of LiFePO_4 grains. The presence of crystalline and evenly distributed carbon enhanced electronic conductivity and rate capability. Moreover, the thickness of carbon coating film also plays an important role in this respect, and more work in this laboratory will be directed towards these issues.

Conclusions

LiFePO_4/C composite was synthesized via a carboxylic acid route by a high-temperature solid-state method. LiFePO_4 coated with 60 wt.% malonic acid as a carbon source can deliver a discharge capacity of 149 mA h g^{-1} at a 0.2 C rate and sustain 222 cycles at 80% of capacity retention. LiFePO_4/C composites with low I_D/I_G ratios can be produced by incorporating carboxylic acid additives before the final sintering process. The Raman peak intensity ratio (I_D/I_G) of the synthesized powders was from 0.907 to 0.935. The presence of excess carbon content between the particles can decrease the charge and discharge capacity. The use of carboxylic acid as a carbon source not only increases the overall conductivity ($\sim 10^{-4} \text{ S cm}^{-1}$) of the material but also prevents particle growth during the final sintering process.

Acknowledgments Financial support for this work was provided by the National Science Council of the Republic of China under contract No. NSC 95-2218-E-008-020.

References

1. Padhi AK, Nanjundaswamy KS, Masquelier C, Okada S, Goodenough JB (1997) *J Electrochem Soc* 144:1609
2. Padhi AK, Nanjundaswamy KS, Goodenough JB (1997) *J Electrochem Soc* 144:1188
3. Andersson AS, Kalska B, Haggstrom L, Thomas JO (2000) *Solid State Ion* 130:41
4. Andersson AS, Thomas JO (2001) *J Power Sources* 97–98:498
5. Andersson AS, Thomas JO, Kalska B, Haggström L (2000) *Electrochem Solid-State Lett* 3:66
6. Zhang SS, Allen JL, Xu K, Jow TR (2005) *J Power Sources* 137:93
7. Hsu KF, Tsay SY, Hwang BJ (2005) *J Power Sources* 146:529
8. Chung SY, Bloking JT, Chiang YM (2002) *Nature* 732:22
9. Wang GX, Bewlay S, Yao J, Ahn JH, Dou SX, Liu HK (2002) *Electrochem Solid-State Lett* 7:503
10. Wang GX, Bewlay S, Needham SA, Liu HK, Liu RS, Drozd VA, Lee J-F, Chen JM (2006) *J Electrochem Soc* 153:A25

11. Yonemura M, Yamada A, Takei Y, Sonoyama N, Kanno R (2004) *J Electrochem Soc* 151:A1352
12. Croce F, Epifanio AD, Hassoun J, Deptula A, Olczac T, Scrosati B (2002) *Electrochem Solid-State Lett* 5:47
13. Parka KS, Sona JT, Chungb HT, Kimc SJ, Leea CH, Kanga KT, Kim HG (2004) *Solid State Commun* 129:311
14. Eftekhari A (2004) *J Electrochem Soc* 151:A1816
15. Park KS, Son JT, Chung HT, Kim SJ, Lee CH, Kim HG (2003) *Electrochem Commun* 5:839
16. Chen Z, Dahn JR (2002) *J Electrochem Soc* 149:A1184
17. Hu Y, Doeff MM, Kostecki R, Finones R (2004) *J Electrochem Soc* 151:A1279
18. Wang GX, Yang L, Bewlay S, Chen Y, Liu HK, Ahn JH (2005) *J Power Sources* 146:521
19. Yamada A, Chung SC, Hinokuma K (2001) *J Electrochem Soc* 148:A224
20. Kwon SJ, Kim CW, Jeong WT, Lee KS (2004) *J Power Sources* 137:93
21. Mi CH, Zhao XB, Cao GS, Tu JP (2005) *J Electrochem Soc* 152:A483
22. Fey TK, Lu TL, Kao HM (2008) *J. Power Sources* (in press)
23. Doeff MM, Hu Y, McLarnon F, Kostecki R (2003) *Electrochem Solid-State Lett* 6:A207
24. Hsu KF, Tsaya SY, Hwang BJ (2004) *J Mater Chem* 14:2690
25. Mi CH, Zhang XG, Zhao XB, Li HL (2006) *J Alloys Compd* 424:327
26. Salah AA, Mauger A, Zaghbi K, Goodenough JB, Ravet N, Gauthier M, Gendron F, Julien CM (2006) *J Electrochem Soc* 153:A1692
27. Tanabe Y, Yamanaka J, Hoshi K, Migita H, Yasuda E (2001) *Carbon* 39:2347
28. Sadezky A, Muckenhuber H, Grothe H, Niessner R, Pöschl U (2005) *Carbon* 43:1731
29. Doeff MM, Wilcox JD, Kostecki R, Lau G (2006) *J Power Sources* 163:180
30. Zhang SS, Allen JL, Xu K, Jow TR (2005) *J Power Sources* 147:234
31. Ho CS, Won IC, Ho J (2006) *Electrochimica Acta* 52:1472
32. Croce F, Nobili F, Deptula A, Lada W, Tossici R, D'Epifanio A, Scrosati B, Marassi R (1999) *Electrochem Commun* 1:605
33. Nobili F, Croce F, Scrosati B, Marassi R (2001) *Chem Mater* 13:1642